Abrupt Onset of Second Energy Gap at Superconducting Transition along the Fermi Arc of Underdoped Bi2212.

Wei-Sheng Lee,[1] K. Tanaka,[1,2] D.H. Lu,[1], T. Sasagawa,[1]
D.J. Scalapino,[3] N. Nagaosa,[4] T.P. Devereaux,[5] Z. Hussain,[2] and Z.-X. Shen,[1*]

[1]Department of Physics, Applied Physics, and Stanford Synchrotron Radiation Laboratory, Stanford University, Stanford, CA 94305, USA
[2]Advanced Light Source, Lawrence Berkeley National Lab, Berkeley, CA 94720, USA
[3]Department of Physics, University of California, Santa Barbara, CA 93106-9530, USA
[4]Department of Applied Physics, University of Tokyo, Bunkyo-ku, Tokyo 113-8656, Japan
[5]Department of Physics, University of Waterloo, Ontario N2L3G1, Canada

*To whom correspondence should be addressed; E-mail: zxshen@stanford.edu.

The temperature dependence of the gap along the Fermi surface of underdoped Bi2212 system is measured by angle-resolved photoemission spectroscopy. Near the nodal region of the Fermi Surface, a gap opens at the superconducting transition temperature T_C, exhibiting a conventional BCS behavior albeit with d-wave shape. This is in sharp contrast to the most studied gap at the antinodal region, which is well known not to exhibit any obvious temperature dependence in its magnitude. This dichotomy leads to a highly non-trivial temperature dependent evolution of the gap along the Fermi surface, providing new insights on the relationship between the su-

perconducting gap and pseudogap. They are distinct, as reflected in the temperature as well as the doping dependence (*1*), but at the same time intimately related as the two gaps merge to form an almost perfect $d-$wave form near optimally doping.

The underdoped regime of the cuprate superconductors is full of surprises. The most mysterious one is the pseudogap, an energy gap which opens at a temperature well above the superconducting transition temperature, T_C (*2,3*). As direct probes of electronic spectra, angle-resolved-photoemission spectroscopy (ARPES) and scanning tunneling spectroscopy (STM) data have shown that the magnitude of the gap evolves continuously across T_C, suggesting that the pseudogap and superconducting gap are of the same origin (*4–7*). In particular, for ARPES spectra taken near the antinodal region, where the gap is maximal and the spectral lineshape shows a strong temperature dependence, the spectral peak position does not show anomaly at T_C (*7*) suggesting that the magnitude of the gap is not correlated with the superconducting transition. The absence of a gap-opening at T_C has been considered as a distinct feature separating the cuprates from conventional superconductors, in which the pairing gap is the order parameter that reflects the onset of the superconducting phase transition (*8*).

Because of its stark contrast to the behavior of the conventional BCS superconducting gap, the pseudogap phenomenology has generated a spirited debate. The proposed ideas range from preformed Coopper pairs (*8,9*), spin pairing (*10*), to competing states (*11–14*). All these theories are consistent with the importance of the phase coherence, as the proximity to Mott insulator state suppresses the superfluid density and thus, the phase stiffness (*9, 15*). However, whether the pseudogap is the precursor of superconducting gap or represents a competing phenomena is an important issue with serious implication for the theory of High-T_C superconductivity.

Aside from earlier ARPES and STM results, a number of other experiments suggest the presence of two energy gaps. These include recent ARPES measurement on heavily underdoped Bi2212 (*1*), Raman spectroscopy (*16, 17*), penetration depth measurements (*18*), Andreev reflection (*19, 20*), intrinsic tunneling (*21*), and femtosecond spectroscopy (*22*). In particular, the latter three indicate the presence of a second energy gap which turns on at T_C. However, these reports of an gap-opening at T_C contain technical uncertainties, for example, possible junction heating in the intrinsic tunneling, (*23*), the indirect nature of femtosceond spectroscopy, and the general difficulty in fabricating tunneling junction in cuprates. This debate of one versus two gaps has been brought to sharper contrast because of recent experiments. (*1, 17, 24–26*). The basic question is again whether the gap seen above T_C is the superconducting gap.

In this paper, with ARPES's unique ability to resolve the electronic states in momentum space, we performed detailed temperature and momentum dependent measurements on underdoped Bi2212 with $T_C = 92$ (UD92K). We discovered a sudden onset of an energy gap at T_C along the Fermi Arc near the nodal region (the diagonal of the Brillouin zone), which remains un-gapped at T_C; this is in contrast with the well-know pesudogap in the antinodal region, which does not exhibit any obvious change in its magnitude across T_C (*4, 28*). This distinct temperature dependence of the gap between the nodal and antinodal region leads to a temperature dependent evolution of the gap function $|\Delta_k(T)|$ *below* T_C. Our data suggest an intricate picture for the energy gap mystery in underdoped cuprates. On the one hand, there are two distinct gaps; one, which turns on at T_C, is the superconducting gap; the other, which develops at a temperature well above T_C, is the pseudogap. On the other hand, there is a intimate relationship between the two gaps. For example, the gap profile of our UD92K sample along the Fermi surface is temperature dependent and smoothly evolves from two gaps into a simple d-wave form at a temper-

ature well below T_C, revealing a mysterious interplay between the superconducting gap and pseudogap.

High quality single crystal of slightly underdoped $Bi_2Sr_2CaCu_2O_6$ with $T_C = 92$ K were selected for the experiments. Angle-resolved photoemission spectroscopy measurements were performed at beamline 5-4 of Stanford Synchrotron Radiation Laboratory (SSRL) with a SCIENTA R4000 photo-electron analyzer. Photons with an energy of 22.7 eV were used to excite the photo-electrons and the total energy resolution was set to 7 meV for the data shown in Fig. 1 and Fig. 3 and 5 meV for the data shown in Fig. 2. To maintain a clean surface, the sample were cleaved *in situ* and measured in a ultra high vacuum chamber with a pressure of better than 7×10^{-11} Torr. (See the section of "Materials and Methods" for more details.)

The ARPES spectrum represents the occupied part of the single-particle spectral function, which is distorted near the Fermi energy E_F because of the Fermi-Dirac function cut-off (FD cut-off). An approximate way to removed this distortion effect is to divide the ARPES spectrum by an effective Fermi-Dirac function, which is generated from the convolution of the FD function at the sample temperature with the energy resolution function. One advantage of this procedure is that it reveals the band dispersion above E_F at higher temperatures, where there is an appreciable spectral weight above E_F due to the thermal population. In Fig. 1(a), we plotted the false-color image of the effective Fermi-Dirac function divided spectra along the Fermi surface at three different temperatures for the UD92K sample. As shown in the data taken at above T_C (102K, top row of Fig. 1(a)), the energy band (the high intensity region) clearly disperses across E_F for the cuts C1 to C4, suggesting that above T_C, there is no detectable gap on the Fermi Surface between the node and the intermediate region. In contrast to this gapless Fermi Arc region, the band dispersion near the antinode (C5 to C8) breaks up near E_F indicating

the existence of an energy gap, the well-known pseudogap. We note that this momentum dependence of the pseudogap is consistent with previous data (*4, 5*).

When the system is cooled down from above T_C to below T_C, the magnitude of the gap exhibits a dichotomy in the temperature dependence between the nodal and antinodal regions. At the antinodal region (C8), the magnitude of the gap does not exhibit detectable temperature dependence across T_C, although a sharper peak in the spectrum begins to develop when the temperature is lower than T_C, as illustrated in Fig. 1(c). The lack of temperature dependence of the antinodal gap size was previously considered as evidence that pseudogap is associated with preformed Cooper pairs which lack the phase coherence necessary for superconductivity (*8, 9*). On the other hand, for the FS near the nodal region (C1 to C4), an energy gap opens up right below T_C (82K, the middle row of Fig. 1 (b)), and becomes larger as the system cools down to a temperature well below T_C (10 K, the lowest row of Fig. 1(a).). We note that at 82K, there is appreciable thermal population above T_C, such that the upper branch of the Bogoliubov dispersion can be clearly seen in the raw spectrum for C1-C4, as illustrated in Fig. 1(b). This observation implies that the gap near the nodal region represents a true superconducting gap, since the Bogoliubov band dispersion is an hallmark of the superconducting state when a superconducting gap opens on the Fermi surface.

The left panel of Fig. 2(a) illustrates a detailed temperature dependence of the FD-divided Energy Distribution Curves (EDCs) for UD92K sample near location "A" indicated in the inset of Fig. 2(b). Upon warming up from 20 K to the 103 K, the spectral peak is seen to move closer to E_F, reaching the E_F when the temperature is higher than T_C. This suggests that the superconducting gap at location A vanishes above T_C. In the right panel of Fig. 2(a), symmetrized EDCs are also plotted providing another method to visualize the behavior of the gap at the Fermi crossing point k_F (*5*); consistent with

the FD-divided spectrum, the superconducting gap collapses at T_C. We further tried to extract the gap size from the data by fitting the symmetrized spectra to a model (*28*), which contains a "minimum" set of parameters: the gap size and the lifetime broadening of the quasi-particles (see the section of "Materials and Methods" for details of the fitting). The fitted gap sizes of two different locations near the nodal region are plotted versus temperature in Fig. 2(b). At both locations, the gap gradually decreases as temperature approaches T_C, and vanishes at a temperature close to T_C, following the functional form of $\Delta(T)$ in weak-coupling BCS theory surprisingly well (*27*). This is different from a previous picture for the underdoped cuprates, which suggested that the superconducting gap was well developed at T_C, as if T_C didn't play a role in the energy gap of the single particle spectral function (*4, 28*). Here, on the contrary, our data suggest that near the nodal region, there exists a portion of the Fermi surface where the superconducting gap opens at T_C even for the underdoped system.

Fig. 3(a) shows the fitted gap size of the UD92K data used in Fig. 1 along the Fermi surface in which the temperature dependence of the gap can be roughly sorted into two different groups. One group is the region near the node where the gap is temperature dependent with an onset temperature close to T_C. The other group is associated with the antinodal region, which does not show any obvious temperature dependence across T_C, as reported previously (*4, 28*). We also note that the BCS curves (dashed lines) starts to deviate from the data when moving toward the antinodal region suggesting a smooth transition from one group to the other. With these two rather different temperature variations, an unusual temperature evolution of the gap function $|\Delta_k(T)|$ along the Fermi surface can be sketched. As shown by the 82 K data in Fig. 3(b), the gapless region near the node at above T_C begins to develop a gap consistent with the simplest $d_{x^2-y^2}$ form, $|\cos k_x - \cos k_y|/2$ (indicated by a straight line) at a temperature right below T_C, whereas

the gap near the antinodal region apparently deviates from the d-wave gap developed near the nodal region. Surprisingly, for this doping, when the system is cooled down to a temperature well below T_C, the momentum dependence of the gap on the entire FS is consistent with the simplest $d_{x^2-y^2}$ form. This evolution of the gap function can also be extracted without using a model. In the inset of Fig. 3(b), we plotted the gap size extracted from the peak position of FD-divided spectrum, which exhibits a consistent temperature dependent evolution with Fig. 3(b).

The evolution of the momentum dependence of the gap for the UD92K sample is schematically illustrated in Fig. 3(c). Above T_C, there exists a gapless Fermi arc region near the node; while a pseudogap has already developed near the antinodal region as illustrated by the red curve in Fig. 3(c). When the system is cooled down to a temperature below T_C, a superconducting $d_{x^2-y^2}$ gap begins to open along the near nodal arc region. In the antinodal region, a sharp peak in the spectrum begin to develop, while the gap remains about the same as that above T_C. In addition, the gap profile in this region deviates from the expected simple $d_{x^2-y^2}$ form developed in the Fermi arc region. At a temperature well below T_C, the superconducting gap with the simplest $d_{x^2-y^2}$ form eventually extends across entire Fermi surface. This change of the gap function in the superconducting state ($T < T_C$) is in sharp contrast to the mean field behavior, in which the momentum dependence of the gap should not change with temperature once it is below T_C. Thus, the observed temperature dependent evolution of the gap function implies a profound interplay between the superconducting gap and pseudogap. (*29*)

We also remind the readers that the distinct temperature dependence of the gap in different part of momentum space has been reported in literatures (*5, 28*) with less detailed momentum dependence. We note that the reported data were taken at locations away from the gapless nodal Fermi arc region; thus, the behavior is consistent to that

of C5-C7 shown in Fig. 3(a), whose gaps have already opened at T_C. With information only restricted in this region, the authors concluded that the pseudogap smoothly evolves into the superconducting gap implying that they represent the identical energy scale, the $d-$wave pairing amplitude (*5*). In addition, in this scenario, one should not expect a temperature dependent gap function below T_C, since the gap has already developed at T_C. However, our new finding about a sudden onset of the superconducting gap at T_C near the node and a temperature dependent evolution of the gap function below T_C suggest that the previous conclusion needs to be revised.

We believe that our data is unlikely to be explained within a single gap picture. We are not aware of any single mechanism that would create an energy gap which opens at different temperatures on the same sheet of the Fermi surface. In addition, the temperature dependent evolution of the gap function for the entire FS in the superconducting state ($T < T_C$) seems also very difficult to be reconcile by the single gap picture. Thus, it is more reasonable to conclude that there exists two energy gaps. The energy gap which opens at T_C near the nodal region is associated with the order parameter of the superconducting state; while the psuodogap at the antinodal region is associated with a different mechanism may or may not related to the superconductivity. This is consistent with the two-gap picture derived from the doping dependence measurements on heavily underdoped Bi2212 described in our recent work (*1*). Furthermore, this temperature dependence dichotomy of the nodal and antinodal region due to the presence of two gaps can also explain the disagreements between different experimental probes; some probes, such as Andreev reflection (*20*), maybe more sensitive to the nodal region or the superconducting condensate; thus, they detect a BCS-like temperature dependent superconducting gap. As for the STM data, the momentum integrated spectra are dominated by the antinodal region due to larger phase space. Further, the reported temperature dependence data

were focus on the evolution of the peak at higher bias voltage (*6*), which maybe more sensitive to the antinodal region; thus a temperature independent gap, the pseudogap, is measured. We speculate that a detailed study on the low bias voltage of STM data may provide important information on the behavior of the gap. Raman scattering on the other hand, via its polarization dependence, can be sensitive to the gap in both regions of the Fermi surface (*16, 17*).

What are the relationship between the observed two gaps? On the one hand, the sudden onset of the superconducting gap near the nodal region seems suggest a competing nature with the pseudogap at the antinodal region; on the other hand, the evolution of the gap profile into a simple $d-$wave form at low temperature observed in UD92K sample seems to suggest a intimate relationship between the pseudogap and superconducting gap. Theoretical calculations, in which the pseduogap is ascribed to a charge density wave competing with the superconducting state (*14*), demonstrate a similar temperature dependence and doping dependence of the gap profile shown in this paper and our recent study on heavily underdoped system (*1*). Likewise, theories, which treat pseudogap as preform Cooper pairs, could also exhibit a two-gap behavior. For example, bipolaron theories (*30*) demonstrate a distinct temperature dependent behaviors of two energy gaps, in which one gap open at T_C in a fashion of BCS-like behavior and the other is essentially temperature independent across T_C. More detailed theoretical and experimental studies are needed in order to further clarify whether the pseudogap and superconducting gap are competing or commensal. Nevertheless, the identification of two energy gaps on the Fermi surface directly from single particle spectral function via ARPES shall bring us one step closer to reveal this mystery.

Materials and Methods (For Supporting Materials)

Sample and Experimental Method

Single crystals of $Bi_2Sr_2CaCu_2O_{6+\delta}$ were grown by the floating zone technique. The carrier concentrations of the samples were carefully adjusted by the post annealing procedure. Slightly underdoped samples (UD92K) were prepared by a heat-treatment of the crystals in air at 800 ^oC for 200 hours, followed by rapid quenching to room temperature. The onset temperature of superconducting transition, T_C^{on}, determined by SQUID magnetometry, was 92 K with a transition width less than 1K.

Angle-resolved photoemission spectroscopy measurements were performed at beamline 5-4 of Stanford Synchrotron Radiation Laboratory (SSRL) with a SCIENTA R4000 photo-electron analyzer. For the underdoped 92 K samples, we used photons with an energy of 22.7 eV to excite the photo-electrons. Total energy resolution was set to 7 meV for the data shown in Fig. 1 and Fig. 3, while the data shown in Fig.2(a-b) were measured at an energy resolution of 5meV. The measurements were performed in the $\Gamma - Y$ quadrant in the First Brillouin zone, where the main Fermi surface near the nodal region can be well separated from the replica Fermi surface due to the photo-electron diffraction by the super-modulation of the crystal structure. The temperature fluctuation during our measurement was less than 0.1 K. To maintain a clean surface, the sample were cleaved *in situ* and measured in a ultra high vacuum chamber with a pressure of better than 7×10^{-11} Torr.

We also note that at 22.7 eV both bonding band and antibonding band can be resolved in the data. At the antinodal region, since the antibonding band and replica Fermi surface due to crystal super-modulation mix up and can not be distinguished, we traced the gap along the Fermi surface of bonding band, which was used to make Fig. 3 in our paper.

Fitting the Gap size

To fit the gap size we used the phenomenological model described in Ref (*28*). The self-energy at Fermi crossing point k_F in the superconducting state may be expressed as

$$\Sigma(k_F, \omega) = -i\Gamma + \frac{\Delta^2}{\omega},$$

where Γ is the life time of the quasi-particle related to the width of the spectrum and Δ represents the gap at Fermi crossing point. The spectral function is then calculated according to

$$A(k_F, \omega) = -\frac{1}{\pi} ImG(k_F, \omega) = -\frac{1}{\pi} Im \frac{1}{\omega - \Sigma(k_F, \omega)}.$$

In addition, a Gaussian convolution corresponding to the instrument resolution was applied to the spectral function. Finally, we fit our symmetrized spectra to the convoluted spectral function to obtain the Δ and Γ. In each cut, all available EDCs near the k_F were fitted; the gap size were determined by averaging over the EDCs which are in the proximity of the EDC(s) yielding the smallest fitted gap size.

We note that this model fits reasonably to the data when a clear peak exists in the spectral; thus, all superconducting state data shown in the paper can be fit fairly well by this model. The results we have shown in this paper were obtained by fitting the symmetrized data in the energy range of $\pm$ 70 meV; we have also checked that the choice of the fitting range is not sensitive to the fitted Δ since there is a sharp peak in the spectrum. The error bar for the superconducting gap reported in our paper is set to be $\pm$2 meV, which was estimated by the uncertainty from the fitting procedure ($\sim$ 0.5 meV), uncertainty of fermi energy ($\sim$ 0.5 meV), and another 100 % margin.

To obtain the gap size for the pseudogap in C5-C7, we also used the same model phenomenologically. We found that the fitting is not as robust as it is in the superconducting

gap, especially for the data taken at a location near antinodal region, such as C7. This is because there is no clear peak in the spectrum, as illustrated in the Fig. 1 (c) of our paper. The fitted Δ exhibits larger fluctuation with different choice of the fitting range yielding a larger error bar.

References and Notes

1. K. Tanaka, W. S. Lee, D. H. Lu, A. Fujimori, T. Fujii, Risdiana, I. Terasaki, D. J. Scalapino, T. P. Devereaux, Z. Hussain, Z.-X. Shen, *Science* **314**, 1910 (2006).

2. Tom Timusk and Bryan Statt, *Rep. Prog. Phys.* **62**, 61 (1999).

3. Andrea Damascelli, Zahid Hussain, and Zhi-Xun Shen, *Rev. Mod. Phys.* **75**, 473 (2003).

4. A. G. Loeser, Z.-X. Shen, D. S. Dessau, D. S. Marshall, C. H. Park, P. Fournier, A. Kapitulnik, *Science* **273**, 325 (1996).

5. M. R. Norman, H. Ding, M. Randeria, J. C. Campuzano, T. Yokoya, T. Takeuchi, T. Takahashi, T. Mochiku, K. Kadowaki, P. Guptasarma, and D. G. Hinks, *Nature* **392**, 157 (1998).

6. Ch. Renner, B. Revaz, J.-Y. Genoud, K. Kadowaki, and O. Fischer, *Phys. Rev. Lett.* **80**, 149 (1998).

7. A. G. Loeser, Z.-X. Shen, M. C. Schabel, C. Kim, M. Zhang, and A. Kapitulnik, *Phys. Rev. B*, **56**, 14185 (1997).

8. V. J. Emery and S. A. Kivelson, *Nature* **374**, 436 (1995).

9. Y. J. Uemura, G. M. Luke, B. J. Sternlieb, J. H. Brewer, J. F. Carolan, W. N. Hardy, R. Kadono, J. R. Kempton, R. F. Kiefl, S. R. Kreitzman, P. Mulhern, T. M. Riseman, D. Ll. Williams, B. X. Yang, S. Uchida, H. Takagi, J. Gopalakrishnan, A. W. Sleight, M. A. Subramanian, C. L. Chien, M. Z. Cieplak, Gang Xiao, V. Y. Lee, B. W. Statt, C. E. Stronach, W. J. Kossler, and X. H. Yu, *Phys. Rev. Lett.* **62** 2317 (1989).

10. X. G. Wen and P. A. Lee, *Phys. Rev. Lett.* **76** 503 (1996).

11. Sudip Charkravarty, R. B. Laughlin, Dirk K. Morr, and Chetan Nayak, *Phys. Rev. B*, **63**, 094503 (2001).

12. K.M. Shen, F. Ronning, D.H. Lu, F. Baumberger, N.J.C. Ingle, W.S. Lee, W. Meevasana, Y. Kohsaka, M. Azuma, M. Takano, H. Takagi, and Z.-X. Shen, *Science* **307**, 901 (2005).

13. T. Hanaguri, C. Lupien, Y. Kohsaka, D.-H. Lee, M. Azuma, M. Takano, H. Takagi, J. C. Davis, *Nature* **430**, 1001 (2004).

14. L. Benfatto, S. Caprara, C. DiCastro, *Eur. Phys. J. B* **17**, 95 (2000).

15. Y. Wang, L. Li, N. P. Ong, *Phys. Rev. B* 73, 024510 (2006).

16. M. Opel *et al.*, *Phys. Rev. B* **61**, 9752 (2000).

17. M. Le Tacon *et al.*, *Nature Physics* **2**, 537 (2006).

18. C. Panagopoulos, J. R. Cooper, T. Xiang, *Phys. Rev. B* **57**, 13422 (1998).

19. G. Deustcher, *Nature* **397**, 410 (1999).

20. V. M. Svistunov, V. Yu. Tarenkov, A. I. D'Yachenko, and E. Hatta, *JETP Lett. 71*, 289 (2000).

21. V. M. Krasnov, A. Yurgens, D. Winkler, P. Delsing, and T. Claeson, *Phys. Rev. Lett.* **84**, 5860 (2000).

22. J. Demsar, R. Hudej, J. Karpinski, V. V. Kabanov, and D. Mihailovic, *Phys. Rev. B* **63**, 054519 (2001).

23. A. Yurgens, D. Winkler, T. Claeson, S. Ono, and Yoichi Ando, *Phys. Rev. Lett.* **92**, 259702-1(2004).

24. A. Kanigel, M. R. Norman, M. Randeria, U. Chatterjee, S. Souma, A. Kaminski, H. M. Fretwell, S. Rosenkranz, M. Shi, T. Sato, T. Takahashi, Z. Z. Li, H. Raffy, K. Kadowaki, D. Hinks, L. Ozyuzer, J. C. Campuzano, *Nature Physics*, **2**, 447 (2006).

25. T. Valla, A. V. Fedorov, Jinho Lee, J. C. Davis, and G. D. Gu, *Science*, **314**, 1914 (2006).

26. A. J. Millis, *Science* **314**, 1888 (2006).

27. We note that the values of $2\Delta_0(T = 8K)/k_BT_C$ of our data is $\sim$9.3, which is still much larger than the value $\sim$4.12 predicted by weak-coupling d-wave BCS theory.

28. M. R. Norman, M. Randeria, H. Ding, and J. C. Campuzano, *Phys. Rev. B*, **57**, R11093 (1998).

29. We comment that this smooth evolution into a simple $d-$wave form at low temperature only occur when the magnitude of the pseudogap is comparable to that of the superconducting gap, which happen to be near the optimal doping for Bi2212 system. As for more underdoped Bi2212, we have shown that the extrapolated superconducting gap at the antinode from the nodal $d-$wave gap is smaller than the pseudogap at

the antinodal region at low temperature (*1*); therefore, the gap profile at our lowest reachable temperature is "U" shape instead of a simple $d-$wave form.

30. A. S. Alexandrov and A. F. Andreev, cond-mat/0005315.

31. W.S. Lee thank T. K. Lee for insightful discussions. ARPES experiments were performed at Stanford Synchrotron Radiation Laboratory which is operated by the Department of Energy Office of Basic Energy Science under contract DE-FG03-01ER45929-A001.

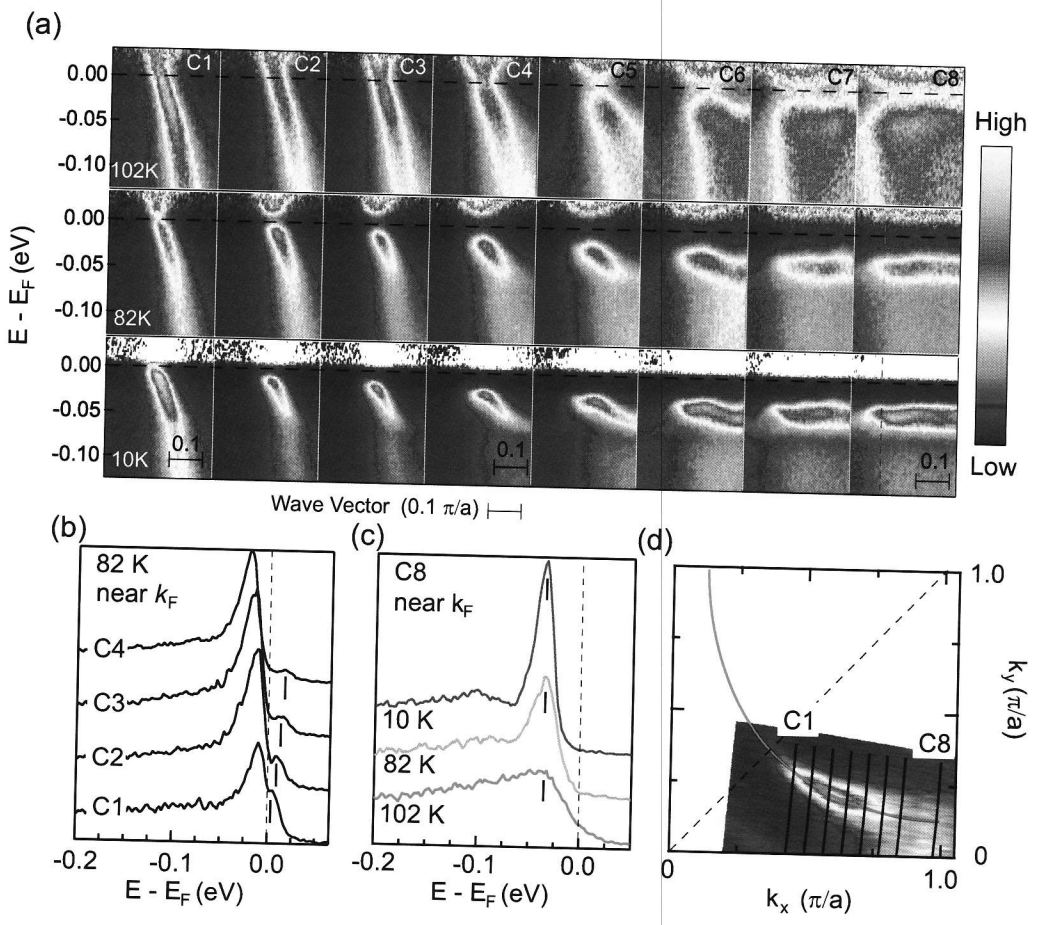

Figure 1: The temperature and momentum dependence of the low energy excitations in slightly underdoped Bi2212 (T_C=92K). (a) The image plots of the Fermi-Dirac function divided ARPES spectrum taken at three different temperatures (10K, 82K, and 102K) at several different locations along the Fermi Surfaces. The momentum positions are plotted as the black lines in (d) with the FS mapping generated by integrating the raw spectrum taken at 102K within an energy window of ± 10 meV around Fermi energy. The intensity of the map is not symmetric with respect to the nodal line (the dashed line) because of the ARPES matrix element effect. (b) Raw EDCs near Fermi crossing point k_F for C1-C4 at 82K. The short vertical lines indicate the thermally-populated, partially occupied Bogoliubov band above E_F. The Bogoliubov band dispersion is a signature of the superconducting gap. (c) Raw EDCs near k_F of C8. A sharp peak in the spectrum can be observed right below T_C, although the gap size remains about the same.

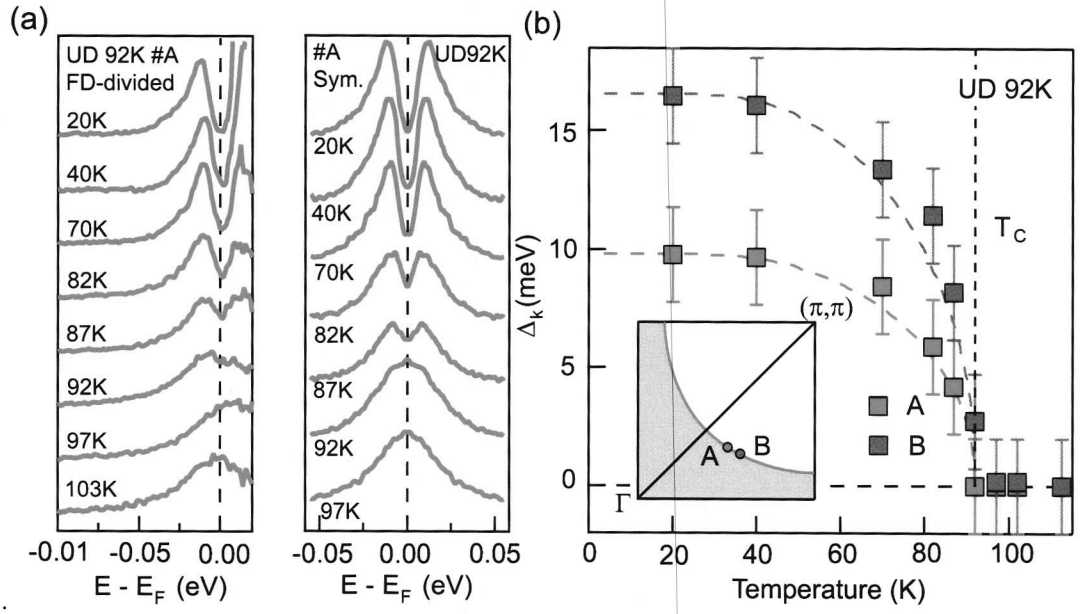

Figure 2: Detailed temperature dependence of the superconducting gap for underdoped Bi2212 with T_C=92K, respectively. (a) The Fermi-Dirac Function divided spectra (left panel) and symmetrized spectra (right panel) for T_C=92K samples, respectively. Both methods indicate the gap vanishes near T_C. (b) The temperature dependence of the gap size for T_C=92K samples, respectively, at momentum positions close to the node, as indicated in the insets. The gap size was obtained by fitting the symmetrized spectra to a phenomenological model proposed in Ref (*28*). The dashed lines show the temperature dependence of the superconducting gap predicted in weak-coupling BCS theory and serve as a guide-to-the-eye for our data. We note that the $\Delta_k(T = 0)$ for the BCS curves are adjusted independently in order to match the data at different locations.

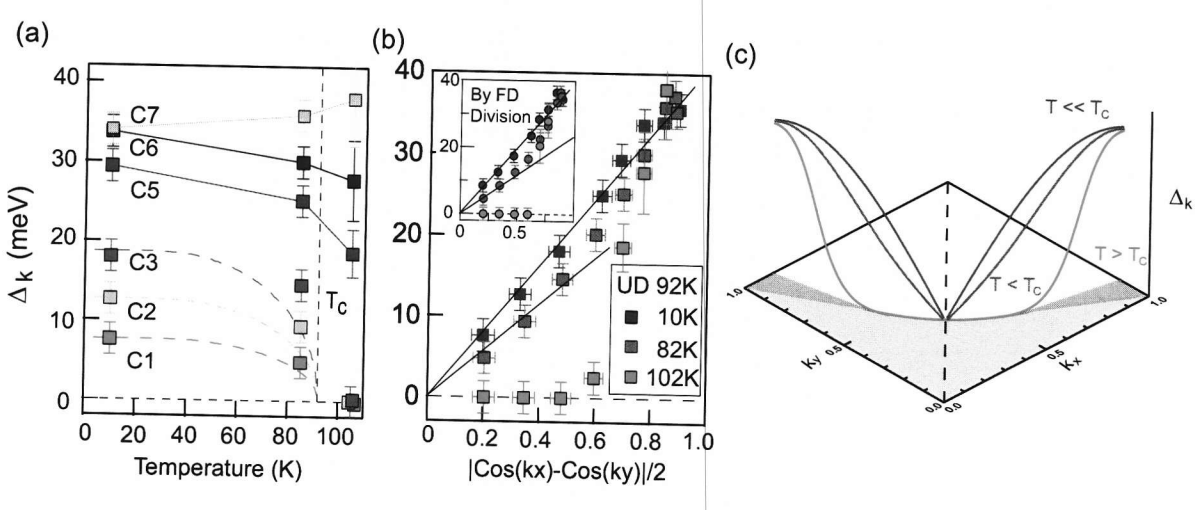

Figure 3: Temperature dependence of the gap profile for Bi2212 UD92K sample. (a) The fitted gap values versus temperature for selective momentum locations along the Fermi surface, which are defined in Fig. 1 (b). The dashed lines show the temperature dependence expected from weak- coupling BCS theory. (b) The fitted gap versus the simplest $d_{x^2-y^2}$ function, $|\cos k_x - \cos k_y|/2$. The lines are guides-to-the-eyes indicating the expected momentum dependence of $d_{x^2-y^2}$ form. The inset shows the same plot with the gap determined from the Fermi-Dirac function divided spectrum. (c) An illustration of the gap profile evolution for UD92K sample from above T_C to below T_C.